INFECTION AND IMMUNITY, July 2006, p. 4282–4294 Vol. 74, No. 7
0019-9567/06/$08.00+0 doi:10.1128/IAI.01714-05

Phenotypic and Functional Characterization of Vaginal Dendritic Cells in a Rat Model of *Candida albicans* Vaginitis

Flavia De Bernardis,[1] Roberta Lucciarini,[2] Maria Boccanera,[1] Consuelo Amantini,[2] Silvia Arancia,[1] Stefania Morrone,[3] Michela Mosca,[2] Antonio Cassone,[1] and Giorgio Santoni[2]*

Department of Infectious Parasitic and Immune-Mediated Diseases, Istituto Superiore di Sanità, Rome, Italy[1]; Department of Experimental Medicine and Public Health, University of Camerino, Camerino, Italy[2]; and Department of Experimental Medicine and Pathology, University of Rome La Sapienza, Rome, Italy[3]

Received 20 October 2005/Returned for modification 10 November 2005/Accepted 12 April 2006

This study analyzes the phenotype of vaginal dendritic cells (VDCs), their antigenic presentation and activation of T-cell cytokine secretion, and their protective role in a rat model of *Candida* vaginitis. Histological observation demonstrated a significant accumulation of OX62$^+$ VDCs in the mucosal epithelium of *Candida albicans*-infected rats at the third round of infection. We identified two subsets of OX62$^+$ VDCs differing in the expression of CD4 molecule in both noninfected and *Candida*-infected rats. The OX62$^+$ CD4$^+$ subset of VDCs displayed a lymphoid cell-like morphology and expressed the T-cell antigen CD5, whereas the OX62$^+$ CD4$^-$ VDC subset exhibited a myeloid morphology and was CD5 negative. *Candida* infection resulted in VDC maturation with enhanced expression of CD80 and CD134L on both CD4$^+$ and CD4$^-$ VDC subsets at 2 and 6 weeks after *Candida* infection. CD5$^-$ CD4$^-$ CD86$^-$ CD80$^-$ CD134L$^+$ VDCs from infected, but not noninfected, rats spontaneously released large amounts of interleukin-12 (IL-12) and tumor necrosis factor alpha, whereas all VDC subsets released comparable levels of IL-10 and IL-2 cytokines. Furthermore, OX62$^+$ VDCs from infected rats primed naïve CD4$^+$ T-cell proliferation and release of cytokines, including gamma interferon, IL-2, IL-6, and IL-10, in response to staphylococcal enterotoxin B stimulation in vitro. Adoptive transfer of highly purified OX62$^+$ VDCs from infected rats induced a significant acceleration of fungal clearance compared with that in rats receiving naive VDCs, suggesting a protective role of VDCs in the anti-*Candida* mucosal immunity. Finally, VDC-mediated protection was associated with their ability to rapidly migrate to the vaginal mucosa and lymph nodes, as assessed by adoptive transfer of OX62$^+$ VDCs labeled with 5 (and 6-)-carboxyfluorescein diacetate succinimidyl ester.

Vulvovaginal candidiasis, mostly caused by *Candida albicans*, is a common mucosal infection affecting a large proportion of women of child-bearing age (44). There is broad agreement that local rather than systemic immunity plays a critical role (18, 19). This aspect has been previously reported (13) where the accelerated clearing of the infection occurred following immunization in an oophorectomized rat model of *Candida albicans* infection. This was characterized by the increased number of activated CD4$^+$ CD25$^+$ T cells and CD5$^+$ B cells; in vitro proliferation of vaginal lymphocytes in response to *Candida* antigenic stimulation; and the presence of cytokines, namely, interleukin-12 (IL-12), gamma interferon (IFN-γ), and IL-2, and protective antibodies (Abs) against mannan and aspartyl proteinase antigens in the vaginal fluids (13). More importantly, adoptive transfer of vaginal lymphocytes, and in particular purified CD4$^+$ T cells, can protect normal rats from *Candida* infection (42).

Dendritic cells (DCs) are key inducers of both innate and adaptive immunity (2, 4). These cells patrol the tissues, phagocytosing pathogens, and also infected or dying cells. Once they are exposed to inflammatory mediators, pathogens, or both, immature DCs are transformed into mature migratory and stimulatory DCs that migrate with a high efficiency into draining lymph nodes. Here, mature DCs can activate antigen-specific T lymphocytes, ultimately leading to both memory T-cell expansion and differentiation of effector cells, thus providing immediate protection against pathogens in peripheral tissues (26). The interaction of immature DCs with T cells can also induce T-cell anergy and differentiation of regulatory T cells required for the maintenance of self-tolerance (45). The ability of DCs to mediate diverse and almost contradictory functions has been related to their plasticity. This permits them to undergo a complete genetic reprogramming in response to external stimuli, such as inflammatory cytokines and microbial products, namely lipopolysaccharide, lipoteichoic acid, bacterial DNA, and double-stranded viral (21, 37) and fungal (3) RNAs. These are recognized through a variety of innate receptors (Toll-like-, complement-, mannose-fucose, immunoglobulin [Ig] receptors, and lectins) (17, 33, 40, 41). During the maturation process, DCs undergo intermediate maturational stages in which they express, with a strictly defined kinetics, cytokines and cell surface molecules critical for the initiation and control of innate and adaptive immune responses. Several DC subsets have been described in rat lymphoid organs using DC-specific or nonspecific markers. Thus, the presence of two subsets of DCs expressing the rat DC-specific integrin CD103 recognized by the OX62 monoclonal antibody (MAb), CD4$^+$ SIRPα$^+$ CD5$^+$ CD90$^+$ and CD4$^-$ SIRPα$^-$ CD5$^-$ CD90$^{+/-}$, have been described in afferent lymph and spleen (27, 49, 50). Splenic CD4$^+$ DCs express lower levels of CD103 integrin than CD4$^-$ DCs, whereas both subsets express similar levels of

* Corresponding author. Mailing address: Department of Experimental Medicine and Public Health, University of Camerino, via Scalzino 3, 62032 Camerino (MC), Italy. Phone: 39 0737403319. Fax: 39 0737630618. E-mail: giorgio.santoni@unicam.it.

CD11b molecule. Both subsets express substantial levels of major histocompatibility complex (MHC) class II and are negative for CD86 and CD40 molecules, whereas they differ for CD80 expression with substantial levels present on $CD4^+$ DCs and very low levels present on $CD4^-$ DCs. The $OX62^+$ $CD4^+$ and $OX62^+$ $CD4^-$ DC subsets display lymphoid and myeloid features and markers, respectively, suggesting a different ontogeny. Thus, lymphoid tissue-related markers CD90 and CD5 have been demonstrated on the $CD4^+$ DC subset and on a noncytotoxic subset of splenic DCs (49). In addition, a new DC subset, OX62 negative but MHC class II positive ($CD5^+$, $CD90^+$, $CD4^+$, $CD3^-$, $CD11b^-$, $CD11c^-$, $CD161a^+$, $CD200^+$, $CD32^+$, and $CD86^+$), that resembles the plasmacytoid DC has been identified in the rat spleen (24). Finally, in the rat thymus, DCs segregate into $OX41^+$ and $OX41^-$ cells and express CD90, CD161a, and CD103 markers (5, 49).

Beyond their distinct cell surface receptor phenotype, the DC subsets exhibit different functions. Previous studies have shown that $CD4^+$, but not $CD4^-$, DCs are better stimulators of $CD4^+$ and $CD8^+$ T cells in allogeneic mixed leukocyte reaction (MLR) or in soluble antigen (Ag) presentation assays; in fact, $CD4^+$ DCs induce strong proliferation and Th1/Th2 and Tc1 differentiation. $CD4^-$ DCs promote Th1 but not Th2 differentiation and are poor stimulators of $CD8^+$ T cells (27, 50). Moreover, it has been reported (23) that $CD4^-$ $SIRP\alpha^-$ DCs can play a major role in the maintenance of self-tolerance (45) and display a potent cytotoxic activity in vitro against YAC-1 and Jurkat tumor cells (49).

Vaginal tissue does not contain an organized lymphoid tissue, but it appears to be highly responsive to local (18) or distal mucosal immunization with *Candida* antigens (14, 42), so that a protective antimicrobial response at the vaginal level can be easily achieved. The vaginal mucosa is under constant exposure to infectious agents and is consequently surveyed by DCs that are strategically localized in both the stratified squamous epithelial layer and in the submucosal lamina propria ready to take up the antigen and then migrate to the draining lymph nodes where they prime naïve T cells (51).

At present, little is known about the phenotype and role of vaginal dendritic cells (VDCs) in the induction of mucosal immunity against *Candida albicans* infection. Thus, the aim of our study was to evaluate in detail the phenotype of VDCs in noninfected and *C. albicans*-infected rats and to assess their abilities in terms of antigen presentation, activation of T-cell cytokine secretion, and proliferation. Moreover, by adoptive transfer experiments, we evaluated the capability of VDCs to protect normal rats from *C. albicans* infection.

MATERIALS AND METHODS

Microorganisms and growth conditions. The yeast used throughout this study was *Candida albicans* SA-40, originally isolated from the vaginal secretion of women with acute vaginitis (12). For the experimental infection (see below), a stock strain from Sabouraud dextrose agar (Difco Laboratories, Detroit, MI) was grown in YEPD medium (yeast extract, 1%; neopeptone, 2%; dextrose, 2%) that was gently agitated for 24 h at 28°C. The medium was then harvested by centrifugation ($3,500 \times g$), washed, and suspended to the required number of yeast cells (10^7 in 0.1 ml) in saline solution.

Animals. Oophorectomized female Wistar rats (body weight, 80 to 100 g; Charles River Breeding Laboratories, Calco, Italy) ($n = 70$ animals for each experiment) were used in the study. Animal maintenance and care were performed as described elsewhere (10, 12).

Experimental rat vaginitis and immunization protocol. All rats were maintained under pseudoestrus by injection of estradiol benzoate (Amsa Farmaceutici Srl, Rome, Italy). Six days after the first estradiol dose, the animals were inoculated intravaginally with 10^7 yeast cells in 0.1 ml of saline solution. From each animal, the number of cells in the vaginal fluid was counted by culturing 1-μl samples (using a calibrated plastic loop, Disponoic; PBI, Milan, Italy) on Sabouraud agar containing chloramphenicol (50 μg/ml) as previously described (10, 12). Rats were considered infected when at least 1 CFU was present in the vaginal lavage, namely a count of $\geq 10^3$ CFU/ml. Some vaginal samples were also stained by the periodic acid-Schiff-van Gieson method for microscopic examination. This infection was repeated a second and third time, after resolution of each preceding infection by an equal challenge of 10^8 *C. albicans* cells and with an identical estrogen treatment. After the third intravaginal challenge, the infection of the reinfected animal cleared rapidly, as the limit of $<10^3$ CFU/ml was approached at the end of the first week of infection. There were no *Candida* CFU detected by the end of the second week.

Abs. The following mouse anti-rat MAbs were used. Purified anti-CD86 and fluorescein isothiocyanate (FITC) conjugated (clone OX48), anti-CD80 phycoerythrin (PE) conjugated (clone 3H5), purified anti-CD11b (clone OX42), and purified and PE-conjugated anti-OX62 (clone OX62) were from Serotec, Ltd., Oxford, United Kingdom. FITC-conjugated anti-CD4 (clone W3/25); PE-conjugated anti-CD3 (clone G4.18); PE-conjugated anti-CD8α (clone OX8); purified, FITC-, and PE-conjugated anti-CD5 (clone OX19); PE-conjugated anti-class II RT1B (clone OX-6); PE-conjugated anti-T-cell receptor α/β (TCR-α/β) (clone R73); PE-conjugated anti-TCR-γ/δ (clone V65); and purified anti-OX40 ligand (CD134L, clone ATM-2) were purchased from BD Biosciences, San Jose, CA. PE-conjugated goat $F(ab')_2$ fragment anti-mouse antibody (GAM) was purchased from Cappel-Organon Teknika, Turhout, Belgium. Mouse FITC- and PE-conjugated Abs were used as a negative control (Serotec). Biotin-conjugated rabbit anti-mouse (RAM) and tricolor-conjugated streptavidin were supplied from Caltag Laboratories, Burlingame, CA. For histological analysis, a biotinylated goat anti-mouse immunoglobulin G (IgG) $F(ab')_2$ purchased from Santa Cruz Biotechnology Inc., Santa Cruz, CA, was used.

Immunohistochemical analysis. The rats were killed, and the vaginas were removed and immediately fixed with 10% (vol/vol) neutral buffered formalin. After dehydration in a graded ethanol series and clearing with xylene, the material was embedded in paraffin. Eight-micrometer-thick sections were incubated for 30 min with H_2O_2 in order to inhibit endogenous peroxidase and then for 30 min with blocking solution (3% bovine serum albumin [BSA], 0.3% Triton X-100 in phosphate-buffered saline [PBS]). The sections were then incubated overnight at 4°C with the OX62 MAb, washed in PBS, labeled for 1 h with a biotinylated goat anti-mouse secondary Ab, and then incubated for 30 min at room temperature with Vectastain Elite ABC reagent (Vector Laboratories Inc., Burlingame, CA). Finally, the sections were stained with peroxidase substrate solution (diaminobenzidine peroxidase substrate; Sigma, Milano, Italy), counterstained with hematoxylin-eosin, and analyzed with an Olympus BX-51 microscope and analysis software (Olympus Europa GMBH, Hamburg, Germany).

VDC isolation. To elicit a sufficient number of VDCs, we used a schedule consisting of a round of three consecutive infections, with clearing of each preceding infection, as previously described (12, 13, 42). At the end of the third infection, the vagina was aseptically removed from each dead rat; the vaginal tissue was cut longitudinally and minced with a sterile scalpel in a complete medium consisting of RPMI 1640 (Flow Laboratories, Irvine, United Kingdom) supplemented with penicillin (100 IU/ml), streptomycin (100 mg/ml), L-glutamine (2 mM), sodium pyruvate (2 mM), 2-mercaptoethanol (5×10^{-5} M), and 5% heat-inactivated fetal calf serum (FCS), as well as 25 mM HEPES buffer (Life Technology International, Paisley, Scotland). The minced tissues were digested in complete medium supplemented with sterile 0.25% collagenase D (Boehringer, Mannheim, Germany), following incubation in a shaker for 30 min at 37°C. Before, during, and immediately after the incubation period, samples were mixed in a stomacher homogenizer (Lab Blender 400; PBI). After digestion, tissues and cells were filtered through a sterile gauze mesh, washed with RPMI 1640 medium, and twice centrifuged (200 and $540 \times g$, respectively, for 15 min). Later, cells were isolated by centrifugation at $1,700 \times g$ for 10 min on cold isosmotic OptiPrep solution gradient (AXI-SHIELD Poc AS, Norway, Oslo). VDCs, collected from the low-density fraction, were washed once with complete medium at $1,700 \times g$ for 10 min and counted by trypan blue dye exclusion. VDCs were purified by positive magnetic selection. Cells were briefly incubated with a saturating concentration of OX62 MAb (1 μg/10^6 cells) for 30 min at 4°C. After two washes in PBS supplemented with 0.1% BSA, cells were incubated with magnetic beads coated with anti-mouse IgG (Dynal Biotech ASA, Norway, Oslo), at a 3:1 Dynabead/target cell ratio, for 30 min at 4°C on a rotating apparatus. Cells were then placed in the magnetic device (Dynal MPC) for at

least 1 min. The supernatant was gently removed, and the resulting positively selected cells remained attached to the tube wall. These cells were collected by washing with RPMI 1640 with 1% FCS after the tube was removed from the Dynal MPC.

To detach the beads, cells were resuspended in RPMI 1640 medium supplemented with 1% FCS (prewarmed to 37°C) and under gentle rotation incubated with releasing buffer (4 μl releasing buffer/10^7 Dynabeads) for 15 min at room temperature. $OX62^+$ VDCs from noninfected and infected rats were resuspended in RPMI 1640 medium. These were counted and assessed for viability by trypan blue dye exclusion.

PBMC isolation. Heparinized peripheral blood was withdrawn by cardiac puncture from CO_2-anesthetized noninfected Wistar rats. Peripheral blood mononuclear cells (PBMCs) were isolated by centrifugation on a Ficoll-Hypaque (Lymphoprep; Nicamed, Oslo, Norway) gradient. These were washed twice, counted, and finally resuspended at the appropriate concentration in complete medium for the isolation of T cells by fluorescence-activated cell sorting (FACS).

Immunofluorescence, flow cytometric analysis, and cell sorting. Standard methodology was used for single and double immunofluorescence of VDCs. Briefly, 2×10^5 VDCs from noninfected or infected rats at 2 and 6 weeks after the third round of *Candida* infection were suspended in complete medium, pelleted, and incubated with the appropriate Ab or negative control for 30 min at 4°C. After three washes with cold PBS, VDCs were analyzed for their relative fluorescence intensity.

For double immunofluorescence, cells were incubated for an additional 30 min at 4°C with the respective FITC- or PE-conjugated Ab and washed with cold PBS.

The percentage of positively stained cells, determined over 10,000 events, was analyzed by a FACScan cytofluorimeter (Becton Dickinson). The fluorescence intensity was expressed in arbitrary units on a logarithmic scale. The compensation for each fluorochrome was determined by parallel single-color analysis of cells labeled with one of the fluorochrome-conjugated Abs.

Sorting of $OX62^+$ $CD4^+$ and $OX62^+$ $CD4^-$ VDC subtypes was performed with a FACStarPlus sorter (Becton Dickinson) equipped with an Enterprise laser emitting 150 mW at 488 nm. VDCs, previously labeled with FITC-conjugated anti-CD4, underwent two rounds of sorting by gating on fluorescent cells using FACStar Plus software. Purity of sorted $OX62^+$ $CD4^+$ and $OX62^+$ $CD4^-$ VDC subsets was in the range 97 to 99%, as analyzed with Cell Quest software (data not shown). Sorted $CD4^+$ VDCs were stained with PE-conjugated anti-CD80 or anti-CD134L MAb in combination with an anti-CD86 or anti-CD5 MAb, followed by biotin-conjugated RAM IgG (1:50 dilution) and tricolor-conjugated streptavidin. Electronic compensation, to remove spectral overlap, was used between the green and orange fluorescence and the orange and red fluorescence.

Purified $OX62^+$ VDCs were also sorted based on the expression of CD4 and CD80 by VDC staining with FITC-conjugated anti-CD4 and PE-conjugated anti-CD80 as described above. Purity of sorted $OX62^+$, $CD4^+$ $CD80^+$, $CD4^+$ $CD80^-$, and $CD4^-$ $CD80^-$ VDC subsets was about 98%, as analyzed with Cell Quest software (data not shown).

In addition, $CD4^-$ sorted VDCs were double stained with PE-conjugated anti-CD80 and FITC-conjugated anti-CD86. Staining was also undertaken with PE-conjugated anti-CD134L MAb in combination with FITC-conjugated anti-CD5 MAb.

For histological analysis, $CD4^+$ $CD5^+$ and $CD4^-$ $CD5^-$ VDC subsets were sorted from $OX62^+$ VDCs, stained with PE-conjugated anti-CD4 and FITC-conjugated anti-CD5 MAb, and analyzed as described above. Finally, 2×10^7 PBMCs, from noninfected rats, were stained with FITC-conjugated anti-CD4 and PE-conjugated anti-CD3 and sorted as described above. Purity of sorted $CD3^+$ $CD4^+$ T cells was approximately 98% (data not shown).

Cell proliferation. Vaginal DCs from noninfected and infected rats were suspended in complete medium supplemented with the antimycotic mepartricin (amphotericin methyl ester; 50 μg/ml) kindly provided by V. Strippoli, University of Rome "La Sapienza," Rome, Italy. A final concentration of 5×10^5/ml was dispensed into tissue culture-treated plastic 96-well round-bottom microtiter plates (Costar, Cambridge, MA.). One hundred microliters of purified naïve $CD3^+$ $CD4^+$ T cells (5×10^4) was cultured alone or in a combination of 1% paraformaldehyde (in PBS, pH 7.4) and prefixed VDCs (1:1 VDC/T-cell ratio) in a total volume of 200 μl of culture medium in the presence of staphylococcal enterotoxin B (SEB; 1 μg/ml) for 6 days at 37°C in a humidified atmosphere of 5% CO_2. Cell proliferation was evaluated by pulsing the cells with 0.5 μCi per well of [^{3}H]TdR (6.7 Ci/mmol; New England Nuclear, Boston, MA) during the last 6 h of the 6-day culture. The incorporation of [^{3}H]TdR was measured by a standard liquid scintillation counting technique, after harvesting the cells with a Skatron harvester (Skatron, Oslo, Norway). All cultures were run in quadruplicate.

Morphological analysis. Sorted $OX62^+$ $CD4^+$ and $OX62^+$ $CD4^-$ VDC subsets (1×10^5) were cytospun onto a glass slide ($400 \times g$ for 4 min) and air dried for 1 h. Cells were then stained using May-Grünwald Giemsa coloration and examined under a light microscope.

Cytokine release assay. (i) Culture of purified VDCs for cytokine release. A total of 2×10^5 highly purified cells of the $CD4^+$ $CD5^+$ $CD80^+$ $CD86^+$ $CD134L^+$, $CD4^+$ $CD5^+$ $CD80^-$ $CD86^+$ $CD134L^+$, and $CD4^-$ $CD5^-$ $CD80^-$ $CD86^-$ $CD134L^+$ VDC subsets from noninfected and infected rats were dispensed into tissue culture-treated plastic 96-well round-bottom microtiter plates and cultured for 36 h in 200 μl of complete medium supplemented with the antimycotic mepartricin.

(ii) T-cell cytokine production. A total of 5×10^4 purified $CD3^+$ $CD4^+$ T cells from normal Wistar rats were dispensed into tissue culture-treated, plastic, 96-well, round-bottom microtiter plates and then cocultured for 36 h in 200 μl of complete medium, with equal amounts of syngeneic paraformaldehyde-prefixed VDCs, for 5 min at room temperature (1:1 VDC/T-cell ratio), from the noninfected or *C. albicans*-infected rats, in the presence of SEB (1 μg/ml). Supernatants were collected and stored until analysis at −70°C.

(iii) Detection of cytokines in the supernatants by ELISA. The supernatants of VDC subpopulations from noninfected and infected rats were pooled, centrifuged, and assayed for the presence of cytokines, namely IL-2, IL-12, TNF-α, and IL-10. In addition, the supernatants of unstimulated and SEB-stimulated purified $CD3^+$ $CD4^+$ T cells cocultured with syngeneic VDCs isolated from noninfected and infected rats were pooled, centrifuged, and tested for the presence of IL-2, IL-10, IL-6, and IFN-γ. The enzyme-linked immunosorbent assay (ELISA) kits for IL-2, IL-6, IL-10, tumor necrosis factor alpha (TNF-α), IFN-γ, and IL-12 were purchased from Endogen, Searchlight, Pierce Biotechnology, Inc., Rockford, IL, and Biosource International, Camarillo, CA, respectively.

Samples (VDC and $CD3^+$ $CD4^+$ T-cell supernatants) and the control were added to wells precoated with immobilized specific Abs. Each sample consisted of a volume of 50 ml (1:2 diluted), as indicated by the manufacturer's instructions. After thorough washing, a specific enzyme-linked polyclonal Ab was added to the wells. Finally, after a second washing, a substrate solution was added, and the colorimetric reaction was terminated by specific stop solution. Optical densities were read with an automated microreader (Labsystem Multiscan) at 450 nm, and the results, expressed as picograms per milliliter, were compared with the specific standard curve values for each cytokine. The ELISA sensitivities were as follows: 4 pg/ml for IL-2, 16 pg/ml for IL-6, 3 pg/ml for IL-10, 4 pg/ml for IL-12, 5 pg/ml for TNF-α, and 2 pg/ml for IFN-γ.

Adoptive transfer of VDCs. As previously described above, freshly purified $OX62^+$ VDCs were isolated from noninfected and infected rats at the third round of *Candida albicans* infection (13) and separated by cell sorting. VDCs were injected (10^5 cells/rat) intravenously into oophorectomized estradiol-treated Wistar rats. Control rats received the same number of VDCs taken from noninfected animals. After 24 h, all rats were infected with 10^7 cells of *Candida albicans* and the course of infection was followed by CFU counts, as described above.

CFSE cell labeling and short-term migration assay. Freshly purified $OX62^+$ VDCs, collected as described above from rats infected three times with *C. albicans* (13), were labeled with 5 μM of the vital dye 5 (and 6-)-carboxyfluorescein diacetate succimidyl ester(CFSE) as a mixed isomer (Molecular Probes Inc., Eugene, OR) (15) for 15 min at 37°C. After extensive washing in 10% fetal bovine serum–PBS and PBS, VDCs were counted and injected (10^5 cells/rat) intravenously into oophorectomized estradiol-treated rats. After 24 h, all rats were infected with 10^7 *C. albicans* cells as described above. DCs from spleen, iliac, lumbar, and inguinal draining lymph nodes and vaginal mucosa, collected and purified as previously described, were stained with PE-conjugated OX62 MAb, and CFSE fluorescence intensity was analyzed by flow cytometry on $OX62^+$ cells.

Data assessment and statistics. Statistical comparisons among various groups of animals undergoing adoptive transfer were carried out by analysis of variance followed by Bonferroni's multiple t test, and the statistical significance of the differences was set at $P \leq 0.05$ (two tailed). The statistical significance of all other experiments was determined by Student's t test ($P \leq 0.01$).

RESULTS

Increased distribution of $OX62^+$ VDCs in the vaginal tissues of *C. albicans*-infected rats. VDCs have been previously detected in the vaginal mucosal tissue in the mouse (51). We thus evaluated the presence of VDCs in the vaginal tissue of

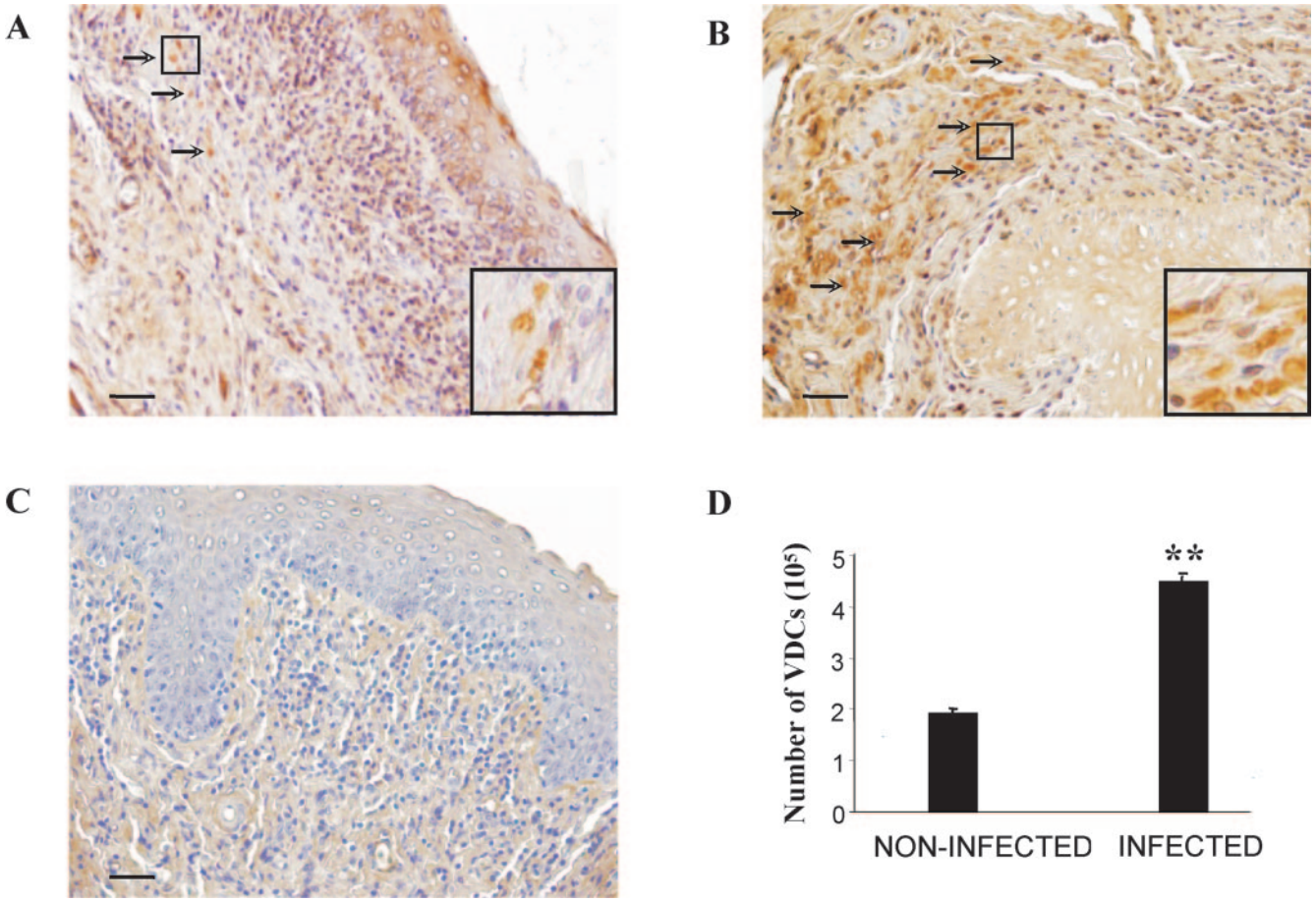

FIG. 1. Vagina sections taken from noninfected (A) or *C. albicans*-infected (B) rats on day 7 after the third round of *Candida albicans* infection. These were stained with the OX62 MAb, followed by biotinylated anti-mouse secondary Ab Vectastain Elite ABC and diaminobenzidine peroxidase substrate, and counterstained with hematoxylin-eosin. (Insets of panels A and B show magnification at ×400.) Panel C shows tissue section stained with an irrelevant MAb as the negative control. Arrowheads indicate $OX62^+$ cells; bars correspond to 50 μm. The total $OX62^+$ VDC numbers from noninfected and infected rats were evaluated by enumeration of $OX62^+$ cells recovered (D). Data represent the total number of VDCs ± standard error of one out of three separate experiments. Statistical significance was determined by comparing the number of $OX62^+$ VDCs from noninfected versus infected rats. **, $P \leq 0.01$ by Student's *t* test.

noninfected and *C. albicans*-infected rats by immunohistochemical analysis using the OX62 MAb. $OX62^+$ VDCs were found in the vaginal mucosa on both noninfected (Fig. 1A) and infected rats (Fig. 1B), after the third round of *Candida* infection, with a higher number of $OX62^+$ VDCs observed in the infected vaginal mucosa. These results were confirmed by a quantitative analysis of the isolated VDC population, which evidenced a significantly higher number of $OX62^+$ VDCs in the vaginal tissue from infected rats compared to those recovered from the vagina of noninfected rats (about 4.5 versus 1.9×10^5/rat) (Fig. 1D).

Phenotypic characterization of VDCs from noninfected and *C. albicans*-infected rats. VDCs were separated from noninfected and infected rat vaginal tissues by positive selection using the OX62 MAb, which recognizes the rat αE2 integrin chain or CD103 (6, 7). This positive selection method did not affect the DC maturation/activation status (50; data not shown). Based on the heterogeneity of the OX62 expression, two major subsets of VDCs were identified in noninfected rats. The main subset (approximately 70%) was $OX62^{high}$ (mean fluorescence intensity [MFI], 753.8) and the minor subset (approximately 30%) was $OX62^{low}$ (MFI, 54.1) (Fig. 2A). Conversely, all the VDCs from infected rats showed a more homogenous phenotype (Fig. 2B), namely $OX62^{high}$ (MFI, 806.1). Rat $OX62^+$ $CD4^+$ and $OX62^+$ $CD4^-$ subtypes have been previously reported in the spleen and pseudoafferent intestinal lymph (27, 49, 50). Thus, we evaluated whether the CD4 antigen was differentially expressed on $OX62^+$ VDCs from noninfected and *C. albicans*-infected rats. On the basis of the CD4 and OX62 expression, we observed the presence of four distinct VDC subsets in noninfected rats: $OX62^{high}$ $CD4^-$ (20%), $OX62^{high}$ $CD4^{high}$ (48%), $OX62^{low}$ $CD4^-$ (24%), and $OX62^{low}$ $CD4^{high}$ (8%). In total, about 56% of $OX62^+$ cells were also $CD4^+$ and the remaining cells (44%) were $CD4^-$ (Fig. 2C). *C. albicans* infection substantially modified the VDC phenotype. Based on the expression of CD4 on $OX62^{high}$ VDCs (Fig. 2D), we could identify two distinct subsets: $OX62^{high}$ $CD4^-$ (45%) and $OX62^{high}$ $CD4^{high}$ (55%). We also analyzed the expression of the T-cell antigen CD5 on both $OX62^+$ VDC subsets from noninfected and infected rats. We

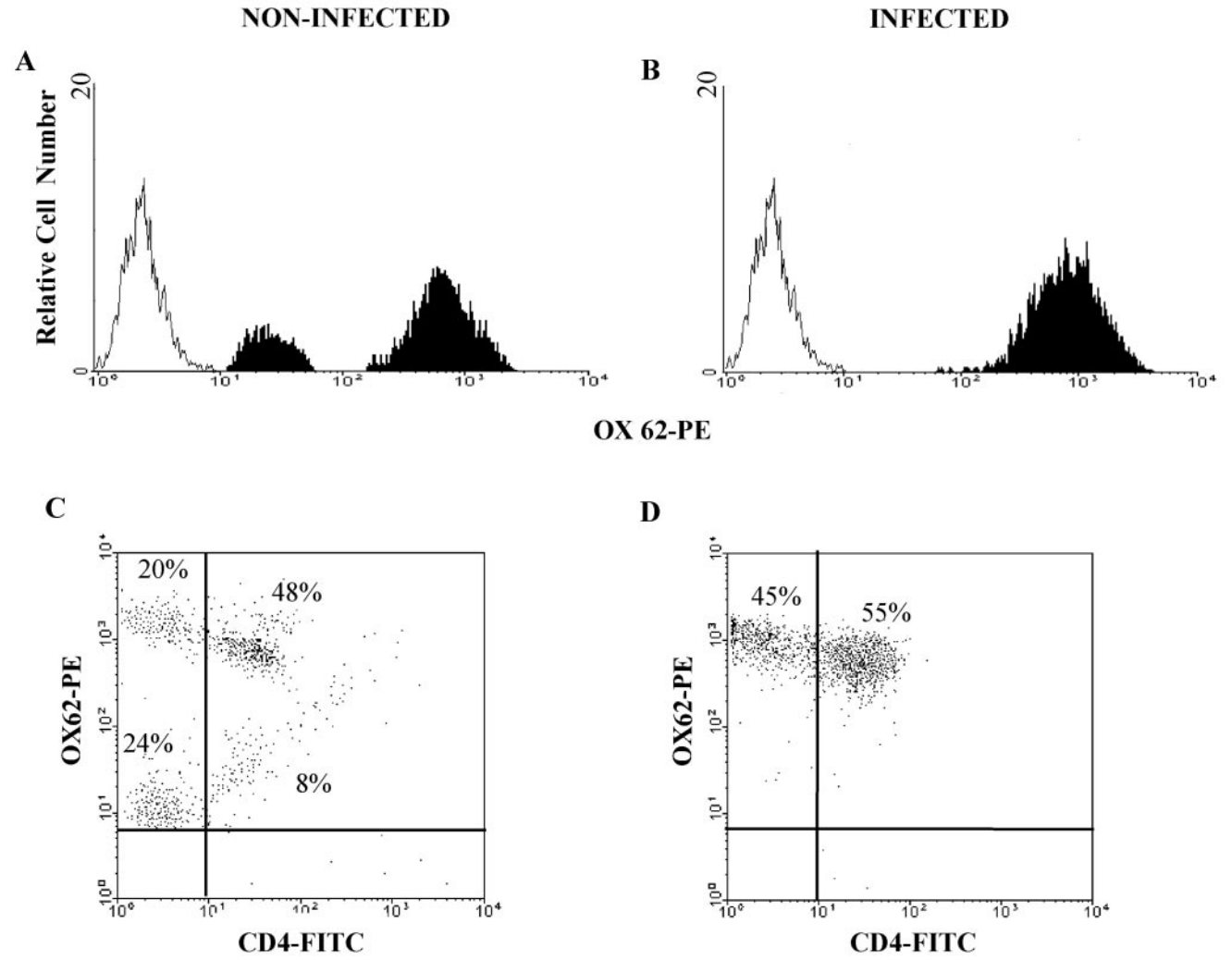

FIG. 2. Expression of OX62 and CD4 molecules on VDCs from noninfected and infected rats. The expression of OX62 on positively selected VDCs from noninfected (A) and infected (B) rats was evaluated by immunofluorescence and FACS analysis using a PE-conjugated OX62 MAb (filled histograms) or with an isotype-matched control Ab (open histograms). The data shown are for three separate experiments, expressed as MFI. VDCs were double stained with FITC-conjugated anti-rat CD4 and PE-conjugated OX62 MAbs and were analyzed by FACS. The data shown are for three separate experiments; the numbers in the upper right corner of the cytograms refer to the percentage of positive cells from noninfected (C) and infected (D) rats.

found that the $OX62^+$ $CD4^+$ subset of VDCs also expressed the T-cell antigen CD5, suggesting the lymphoid origin of this population, whereas the $OX62^+$ $CD4^-$ subset was $CD5^-$ (Table 1).

The morphology of freshly isolated $OX62^+$ $CD4^+$ $CD5^+$ and $OX62^+$ $CD4^-$ $CD5^-$ sorted VDCs was evaluated by cytospin and May-Grünwald Giemsa staining. The $OX62^+$ $CD4^-$ $CD5^-$ VDCs displayed a myeloid cell-like morphology, with a large cytoplasm containing several vesicles (Fig. 3, left panel). In contrast, most of the $OX62^+$ $CD4^+$ $CD5^+$ VDCs had a smaller nucleus and a small cytoplasm containing fewer vesicles (Fig. 3, right panel).

In addition, as OX62 MAb can also recognize some T cells, the expression of TCR-γ/δ, TCR-α/β, and CD8α on noninfected and infected $OX62^+$ VDCs was evaluated in order to rule out the presence of contaminating T cells (6, 7). Both

TABLE 1. Phenotype of VDC subsets[a]

MAb subset	MFI (mean ± SD)[b]			
	$OX62^+$ $CD4^+$		$OX62^+$ $CD4^-$	
	Noninfected	Infected	Noninfected	Infected
CD5	99.1 ± 4.3	126.1 ± 3.2*		
TCR-α/β				
TCR-γ/δ				
CD8α				
CD11b	16.4 ± 1.2	63.5 ± 2.9*	9.7 ± 0.9	106.2 ± 3.9*
Class II RT1B	6.6 ± 0.9	27.7 ± 1.2*	24.9 ± 1.3	72.9 ± 2.7*
CD80		49.9 ± 2.0*		
CD86	17.3 ± 0.9	555.5 ± 8.9*		
OX40L	2.0 ± 0.2	62.8 ± 1.3*		537.4 ± 10.0*

[a] Freshly isolated $OX62^+$ VDCs from noninfected and *C. albicans*-infected rats were double stained with FITC- or PE-conjugated rat anti-CD4 and FITC- or PE-conjugated MAbs against the molecules listed in the left column.

[b] Data are expressed as the MFI on gated $CD4^+$ and $CD4^-$ VDC subsets, corrected by subtracting the MFI of the isotype control Abs and are the mean ± standard deviation (SD) of three separate experiments. Statistical analysis was performed by comparing the MFIs of $OX62^+$ $CD4^+$ and $OX62^+$ $CD4^-$ VDCs from noninfected versus infected rats. *, $P < 0.01$ by Student's *t* test.

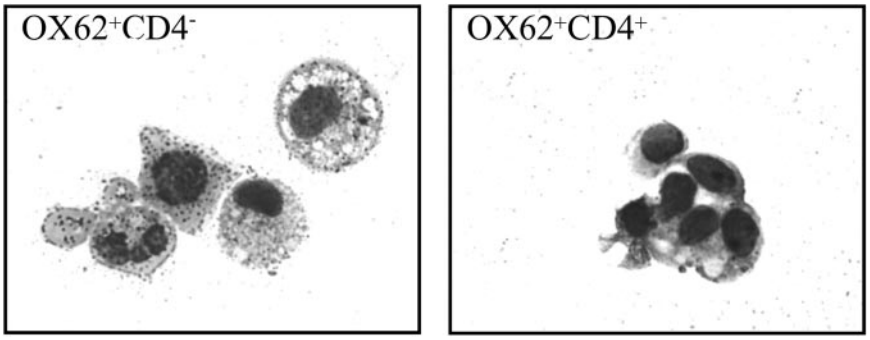

FIG. 3. Morphology of $OX62^+$ $CD4^+$ and $OX62^+$ $CD4^-$ VDC subsets from *C. albicans*-infected rats. Freshly isolated $OX62^+$ VDCs were stained with FITC-conjugated anti-rat CD4 MAb and sorted by FACS. The purity of both $OX62^+$ $CD4^+$ and $OX62^+$ $CD4^-$ subsets was greater than 98%. $CD4^+$ and $CD4^-$ VDC subpopulations were cytospun onto the glass slides, air dried, stained using May-Grünwald Giemsa coloration, and analyzed by Olympus BX-51 microscope (magnification, ×400).

$OX62^+$ $CD4^+$ and $OX62^+$ $CD4^-$ VDCs were negative for TCR-γ/δ, TCR-α/β, and CD8α (Table 1).

***C. albicans* infection induces VDC maturation.** To investigate whether *C. albicans* infection could induce maturation of VDCs, the expression of CD11b and MHC class II RT1B, as well as that of CD80, CD86, and CD134L costimulatory molecules, was evaluated on both $OX62^+$ $CD4^+$ and $OX62^+$ $CD4^-$ subsets from noninfected and infected rats at 2 weeks after infection by immunofluorescence and FACS analysis.

Both $OX62^+$ $CD4^+$ and $OX62^+$ $CD4^-$ VDC subsets from noninfected rats displayed an immature phenotype. Hence, no CD80 or CD86 expression, negligible CD134L expression, and low levels of CD11b and MHC class II molecules were found on $CD4^-$ VDCs (Table 1); similarly, no CD80 and CD134L and low levels of CD11b, CD86, and MHC class II molecules were observed on the $CD4^+$ VDC subset (Table 1). In contrast, a moderate increase in MHC class II and CD11b levels (4-fold) and a very strong increase in CD86 (32-fold) and CD134L (31-fold) expression were detected on the $CD4^+$ VDC subset from infected rats, suggesting that VDCs undergo maturation in response to *C. albicans* infection. Moreover, moderate induction of CD80 expression, substantial increase of MHC class II (3-fold) and CD11b (11-fold) molecules, and very strong induction of CD134L expression were evident on the $CD4^-$ VDC population from infected rats.

In order to analyze more in depth the expression of costimulatory molecules, namely CD80, CD86, and CD134L, we performed three-color immunofluorescence and FACS analysis on sorted $OX62^+$ $CD4^+$ and $OX62^+$ $CD4^-$ VDCs from infected rats at different time points after the third round of *Candida* infection. At 2 weeks after infection, we found that about 34% of $CD4^+$ VDCs were $CD80^-$ $CD86^+$, 66% were $CD80^+$ $CD86^+$ (Fig. 4A), about 62% were $CD134L^+$, and 38% were $CD134L^-$ (Fig. 4B). Furthermore, we observed that $CD4^-$ VDCs were negative for both CD80 and CD86 molecules (Fig. 4E) and positive for CD134L expression (45%) (Fig. 4F and Table 2). Finally, with the use of CD5 antigen, which completely overlapped with CD4 expression, we could demonstrate that $CD4^+$ $CD5^+$ $CD80^+$ $CD86^+$ VDCs were $CD134L^+$ (36%) (Fig. 4C and Table 2), whereas the $CD4^+$ $CD5^+$ $CD80^-$ $CD86^+$ VDCs also lack CD134L (19%) (Fig. 4D and Table 2). In addition, the analysis of MFI shows that the levels of expression of CD80 and CD134L are maintained or even increased on both $CD4^+$ (MFI, CD80 = 43.2 and CD134L = 176.1) and $CD4^-$ (MFI, CD80 = 813.6 and CD134L = 855.2) VDC subsets at 6 weeks after *Candida* infection.

Finally, the analysis of the distribution of $CD80^+$ and $CD134L^+$ subpopulations within the $CD4^+$ and $CD4^-$ VDC subsets shows that the percentage of $CD4^+$ $CD80^+$ $CD134L^+$ VDCs progressively increases (63%) and a subset of $CD4^-$ VDCs expressing both CD80 and CD134L (16%) is observed at later times of *C. albicans* infection, suggesting that CD134L and CD80 costimulatory molecules are differentially regulated during infection (Table 2).

Release of IL-12, IL-2, TNF-α, and IL-10 cytokines by VDCs from *C. albicans*-infected rats. As previously reported (13, 17, 32, 42), the development of Th1-predominant protective immunity in candidiasis is clearly dependent on the production of IL-12 and TNF-α; however, low levels of IL-10 also seem to be required for maintaining a long-lasting Th1 immunity to the fungus (29, 31). Furthermore, DC-derived IL-2 production has been recently reported in mice (21, 22). We therefore examined the spontaneous release of IL-2, IL-12, TNF-α, and IL-10 by highly purified different $OX62^+$ VDC subsets ($CD4^+$ $CD5^+$ $CD80^+$ $CD86^+$ $CD134L^+$, $CD4^+$ $CD5^+$ $CD86^+$ $CD80^-$ $CD134L^-$, and $CD4^-$ $CD5^-$ $CD80^-$ $CD86^-$ $CD134L^+$) from infected rats.

Cell supernatants from noninfected and infected VDCs were harvested at 36 h of culture (Table 3). The $CD4^-$ VDCs produced a larger amount of the proinflammatory cytokines TNF-α and IL-12 compared to the $CD4^+$ VDC subset, whereas no major differences were observed with regard to the release of IL-10 and IL-2. No significant levels of IL-12, TNF-α, IL-2, and IL-10 were found in the supernatants of VDCs from noninfected rats (data not shown). These results indicate that *C. albicans* infection stimulates the production of cytokines, including IL-12, TNF-α, IL-2, and IL-10, by VDCs, being the inflammatory cytokines preferentially produced by the $CD4^-$ $CD5^-$ $CD80^-$ $CD86^-$ $CD134L^+$ VDC population.

Ability of VDCs from *C. albicans*-infected rats to induce naive $CD4^+$ T-cell proliferation in response to SEB. To assess the ability of VDCs from *C. albicans*-infected rats to activate T cells in vitro, VDCs from noninfected and infected rats were

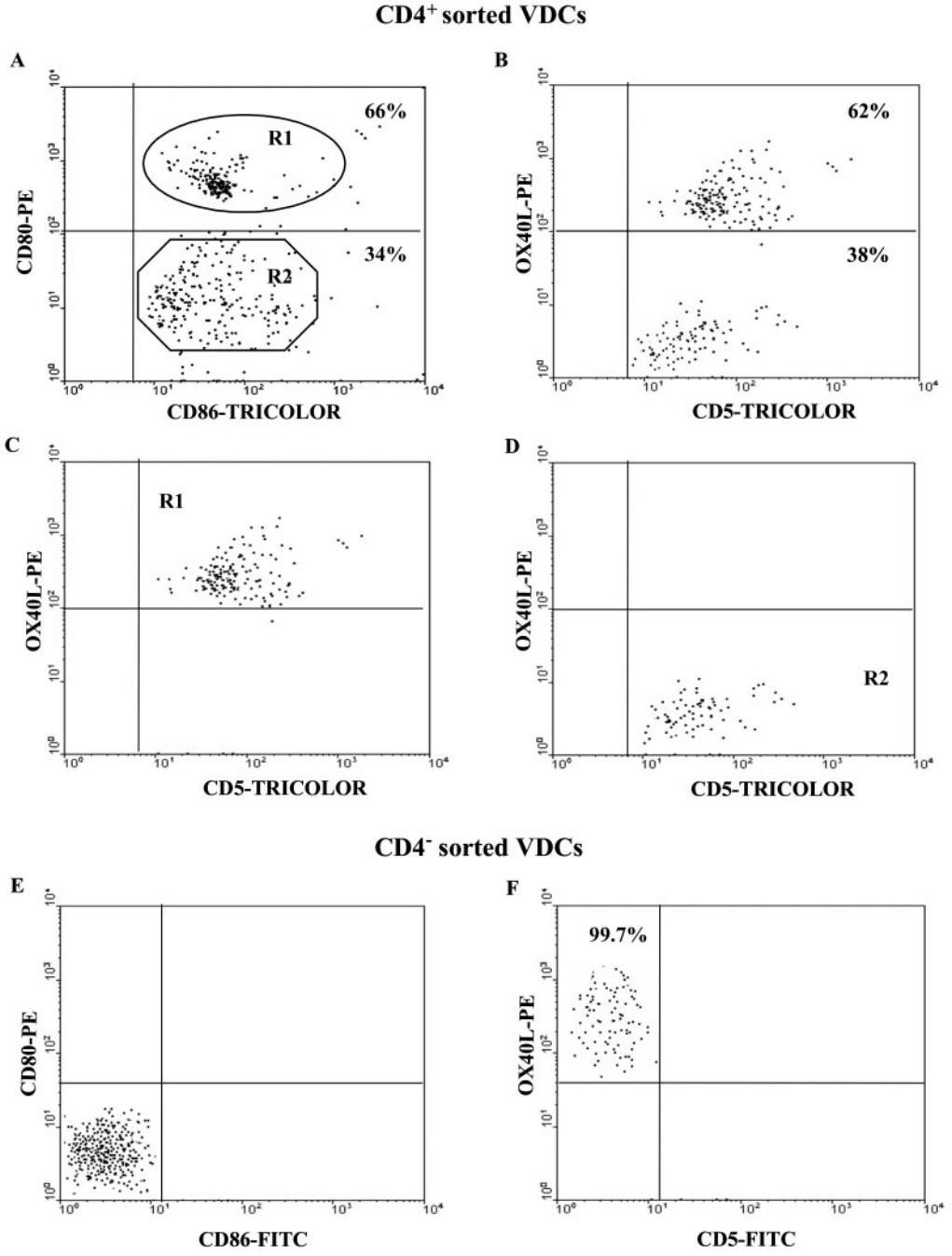

FIG. 4. Phenotypic characterization of freshly isolated OX62$^+$ CD4$^+$ and OX62$^+$ CD4$^-$ VDC subsets from *C. albicans*-infected rats. Highly purified OX62$^+$ VDCs from infected rats were stained with FITC-conjugated anti-rat CD4 and sorted by FACS. Sorted CD4$^+$ (A and B) and CD4$^-$ (E and F) VDCs (97 to 99% pure) were stained with PE-conjugated anti-rat CD80 or OX40L MAb and anti-rat CD86 or anti-rat CD5 MAb, followed by biotin-RAM and tricolor-conjugated streptavidin, and were analyzed by flow cytometry. Panels C and D show the expression of CD5 and CD134L antigens on the CD86$^+$ CD80$^+$ (A, gate R1) and CD86$^+$ CD80$^-$ (B, gate R2) CD4$^+$ sorted VDCs analyzed by CELLQuest software. Data are shown for two separate experiments; the numbers in the upper and lower right corners of the cytograms refer to the percentages of positive cells.

cocultured with sorted peripheral blood CD3$^+$ CD4$^+$ T cells (1:1 VDC/T-cell ratio) from noninfected syngeneic rats in the presence of SEB (1 μM/ml). The T-cell stimulatory activity of VDCs from noninfected and infected rats was evaluated by assessing SEB-stimulated cytokine release in culture supernatant at 36 h and SEB-stimulated T-cell proliferation at 6 days. The results showed that VDCs from infected rats induced the release of high levels of IL-2, IFN-γ, and IL-6 and low levels of IL-10 by T cells in response to SEB stimulation (Fig. 5A). No cytokine release by T cells in the absence of SEB and by

TABLE 2. Distribution of distinct VDC subsets during *C. albicans* infection[a]

VDC subpopulation	% of positive cells at wk postinfection[b]:		
	0	2	6
$CD4^+$ $CD5^+$ $CD86^+$	56 ± 2	55 ± 3	63 ± 2
$CD80^-$ $CD134L^-$	56 ± 2	19 ± 1	0
$CD80^+$ $CD134L^+$	0	36 ± 2	63 ± 2
$CD4^-$ $CD5^-$ $CD86^-$	44 ± 1	45 ± 3	37 ± 2
$CD80^-$ $CD134L^-$	42 ± 2	0	0
$CD80^+$ $CD134L^+$	0	0	16 ± 1
$CD80^-$ $CD134L^+$	2 ± 1	45 ± 3	21 ± 2

[a] Highly purified $OX62^+$ $CD4^+$ and $OX62^+$ $CD4^-$ VDCs from noninfected and *C. albicans*-infected rats at 2 and 6 weeks after the third round of infection were stained with PE-conjugated anti-CD80 or anti-CD134L MAb in combination with an anti-CD86 or anti-CD5 MAb followed by biotin-conjugated RAM IgG (1:50 dilution) and tricolor-conjugated streptavidin.
[b] Data are from two separate experiments.

TABLE 3. Cytokine release in VDC subpopulations[a]

VDC subpopulation	Cytokine expression (pg/ml)[b]			
	IL-10	TNF-α	IL-12	IL-2
$CD4^+$ $CD86^+$ $CD80^+$ $CD134L^+$	400 ± 28	240 ± 21	250 ± 23	250 ± 22
$CD4^+$ $CD86^+$ $CD80^-$ $CD134L^+$	250 ± 20	150 ± 19	150 ± 20	240 ± 26
$CD4^-$ $CD86^-$ $CD80^-$ $CD134L^+$	360 ± 24	600 ± 30*	550 ± 27*	250 ± 25

[a] A total of 2×10^5 highly purified $OX62^+$, $CD4^+$ $CD5^+$ $CD86^+$ $CD80^+$ $CD134L^+$, $CD4^+$ $CD5^+$ $CD86^+$ $CD80^-$ $CD134L^-$, and $CD4^-$ $CD5^-$ $CD86^-$ $CD80^-$ $CD134L^+$ VDCs from noninfected and *C. albicans*-infected rats were cultured in complete medium in 96-well plates at 37°C in 5% CO_2. After 36 h, the supernatants were collected. The IL-2, TNF-α, IL-2, and IL-10 release was measured by ELISA.
[b] Results are the mean ± standard deviation of two separate experiments. *, $P \leq 0.01$ by Student's *t* test.

paraformaldehyde-prefixed VDCs was observed (data not shown).

VDCs from infected rats were capable of inducing naïve $CD4^+$ T-cell proliferation in response to SEB. In contrast, VDCs from noninfected rats stimulated neither T-cell cytokine release nor cell proliferation. No proliferative response was observed in the absence of SEB (Fig. 5B).

Overall, these results indicate that, after *Candida albicans* infection, VDCs acquire the ability to stimulate T-cell proliferation and cytokine release in response to SEB superantigen stimulation.

Protection against *C. albicans* vaginal challenge by adoptive transfer of VDCs from infected rats. After three rounds of infection, 1×10^5 $OX62^+$ purified VDCs isolated from *Candida*-infected rats were intravenously injected as a single administration into noninfected rats 24 h before the intravaginal *Candida albicans* challenge. Animals receiving VDCs from noninfected rats were used as a control. Figure 6 shows the kinetics of fungal clearance from rat vagina. Control rats receiving only *C. albicans* cells had the usual course of vaginal infection (12, 13), with high *Candida* burden in the first week of infection followed by a progressive decline of fungal CFU. The same kinetics of infection were shown by the animals that received $OX62^+$ VDCs from noninfected rats. The animals receiving $OX62^+$ VDCs from *C. albicans*-infected rats showed reduced (50%) *C. albicans* CFU counts. There was a rapid and significant acceleration of fungus clearance, starting immediately 1 day after the fungus challenge and persisting for the whole course of the infection. We then tested the ability of VDCs from infected rats to home to the vagina by performing short-term migration experiments using CFSE-labeled VDCs. Forty-eight hours after adoptive transfer, comparable numbers of $OX62^+$ $CFSE^+$ VDCs redistributed both to vaginal mucosa and draining lymph nodes, while a lower percentage was detectable in the spleen (Fig. 7).

These results indicate that adoptively transferred DCs isolated from the vaginal mucosa of *C. albicans*-infected rats can rapidly migrate to the vagina and draining lymph nodes and protect noninfected rats from *Candida* vaginitis.

DISCUSSION

Dendritic cells function as a link between innate and adaptive immunity and are therefore important in the recognition of pathogens. In particular, they play an important role in the induction of T-cell-mediated immune responses to fungi. Fungus-derived factors provide a powerful activation stimulus to DCs, resulting in DC maturation with up-regulation of costimulatory molecules and production of a number of cytokines leading to different T-cell responses (8).

Several reports indicate the ability of splenic murine DCs to trigger T-cell-mediated immune responses in vitro and in vivo protection against *Candida albicans* infections (3, 17, 34, 48). However, no data concerning the phenotype and the functional involvement of DCs isolated from vaginal tissues in the induction of protective mucosal immunity to *Candida* vaginitis have been published.

VDCs are normally present in the murine mucosal and submucosal tissue (51), but whether their presence and maturation/functional state are modified following immunization with repeated boosts of *Candida* infections has not been reported yet. Thus, by immunohistochemical analysis using the OX62 MAb that recognizes the rat αE2 integrin chain or CD103 (6, 7) and enumeration of $OX62^+$ cells infiltrating the vaginal mucosa, we found a marked increase in the $OX62^+$ VDCs in the vaginal tissue of *C. albicans*-infected rats in comparison to noninfected rats (4.5×10^5 versus 1.9×10^5/rat). At present, it is unknown whether this increase is the result of transient expansion of vaginal DCs in situ, DC recruitment from draining lymph nodes in response to *Candida* infection, or both.

Moreover, the analysis of OX62 expression on VDCs provided evidence of the presence of two distinct $OX62^{high}$ and $OX62^{low}$ VDC subsets in noninfected rats, whereas all the VDCs from infected rats showed the $OX62^{high}$ phenotype. Two phenotypically distinct $OX62^{high}$ and $OX62^{low}$ DC subsets, similar to our results, were found in the normal rat spleen by Voisine and coworkers (50). We characterized more in depth the phenotype of $OX62^+$ VDCs, focusing our attention on markers which can discriminate distinct VDCs on the basis of their ontogeny and maturation/activation status. We found that approximately 50% of VDCs from both noninfected and *C. albicans*-infected rats express CD4 and CD5 T-cell antigen. $CD4^+$ $CD5^+$ VDCs resem-

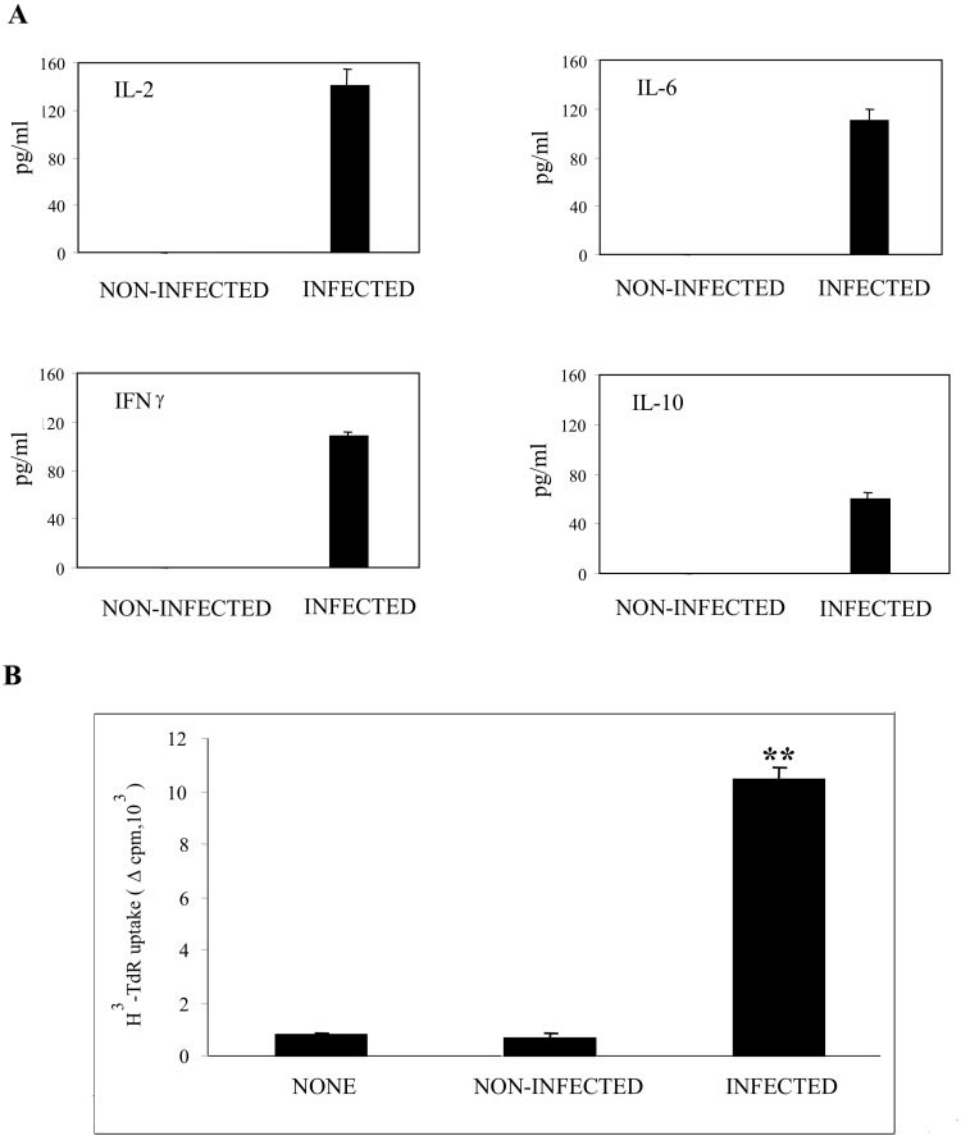

FIG. 5. $OX62^+$ VDCs from *C. albicans*-infected rats trigger $CD3^+$ $CD4^+$ T-cell proliferation and cytokine production in vitro in response to SEB stimulation. (A) Highly purified 1% paraformaldehyde-prefixed $OX62^+$ VDCs (5×10^4) from noninfected and infected rats were cocultured with sorted syngeneic $CD3^+$ $CD4^+$ T cells (CD4 T-cell purity greater than 97%) from noninfected rats at a 1:1 VDC/T-cell ratio in the presence of SEB (1 μg/ml). After 36 h of culture, the supernatants were collected. The IL-2, IFN-γ, IL-6, and IL-10 release was measured by ELISA. Data are expressed as pg/ml. (B) Sorted $CD3^+$ $CD4^+$ T cells (97% pure) from normal rats were cultured alone or with highly purified $OX62^+$ VDCs (5×10^4) from noninfected and infected rats, as described in panel A. After 6 days of culture, T-cell proliferation was assessed by [^{3}H]TdR incorporation. The data shown are the mean ± standard error of three separate experiments. Statistical analysis was performed by comparing the SEB-mediated proliferative response of $CD4^+$ T cells cultured alone or in the presence of $OX62^+$ VDCs from noninfected versus infected rats. **, $P < 0.01$ by Student's *t* test.

ble lymphoid cells, whereas the $CD4^-$ $CD5^-$subset displays a myeloid cell-like morphology, thus suggesting that they may originate from different hematopoietic progenitors. In accordance with our data, two $OX62^+$ populations, $CD4^-$ and $CD4^+$, were isolated by positive selection in the rat spleen (49, 50).

The analysis of CD11b and MHC class II RT1B markers as well as of costimulatory molecules, namely CD86, CD80, and CD134L, indicates that VDCs from noninfected rats are rather immature as the $CD4^+$ subset was negative for the presence of CD80 and CD134L and expressed low levels of CD86, CD11b, and MHC class II RT1B, and the $CD4^-$ cells were $CD86^-$, $CD80^-$, and $CD134L^-$ and exhibited low expression of CD11b and MHC class II RT1B molecules. On the contrary, at 2 weeks after *C. albicans* infection, both $CD4^+$ and $CD4^-$ VDC subsets underwent maturation. This resulted in a significant induction of CD80 and CD134L costimulatory molecules and enhancement of CD86, MHC class II RT1B, and CD11b expression on $CD4^+$ cells, together with induction of only CD134L on $CD4^-$ cells.

Enhanced expression of CD80 and CD134L costimulatory

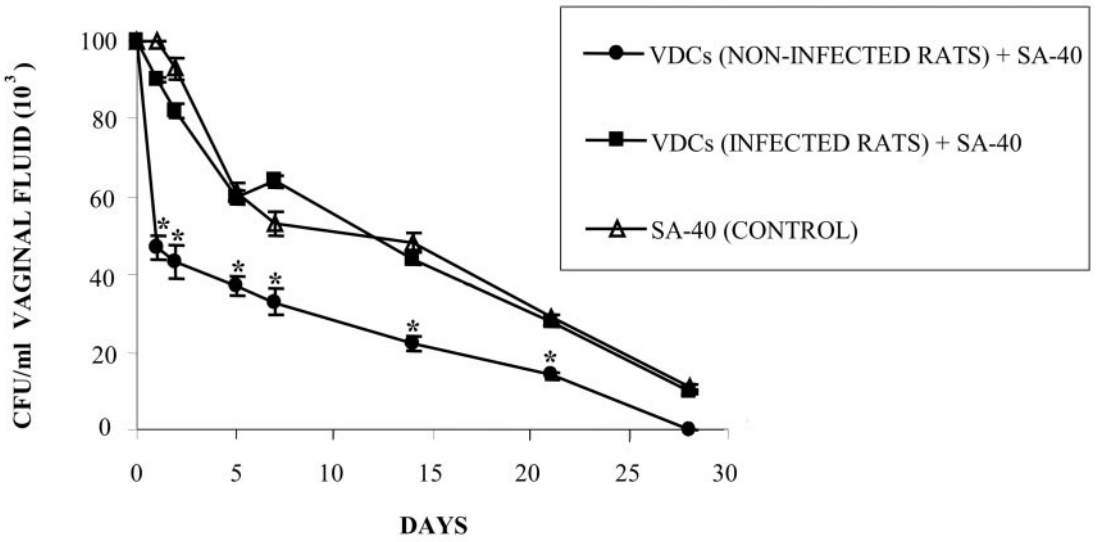

FIG. 6. Kinetics of vaginal infection by *Candida albicans* in oophorectomized, estradiol-treated, noninfected rats intravenously injected (24 h before intravaginal *C. albicans* challenge) with saline (control) or 1×10^5 highly purified $OX62^+$ VDCs from noninfected and infected rats as indicated. Each value represents the mean ± standard error fungal CFU of five rats. Statistical analysis was performed by comparing CFU counts from animals receiving $OX62^+$ VDCs from infected rats with those injected with $OX62^+$ VDCs from noninfected rats or with control rats. *, $P \leq 0.05$ by anlysis of variance and Bonferroni's multiple *t* test.

molecules was maintained on both $CD4^+$ and $CD4^-$ VDC subsets 6 weeks after *Candida* infection, and no major differences in the percentages of $CD4^+$ and $CD4^-$ VDCs were observed. In addition, at later times after infection, we found evidence of a progressive increase in the percentage of $CD4^+$ $CD80^+$ $CD134L^+$ cells and a subset of $CD4^-$ VDCs expressing both CD80 and CD134L (16%). The long-lasting phenotypic changes induced by *C. albicans* infection on VDCs suggest that local stimuli such as proinflammatory cytokines and/or the persistence of low pathogen burden may maintain the mature/activated VDC phenotype.

The CD86 molecule is constitutively expressed on murine DCs and is rapidly up-regulated after activation, whereas CD80 shows a slower kinetics of up-regulation (30). In murine candidiasis, increased expression of CD86 occurs more than that of CD80; this correlates with the enhanced Th1-mediated immune resistance to cutaneous infections with *Candida albicans* (20, 31), although the regulated expression of both costimulatory molecules is required for the development of protective anticandidal immunity (29).

We first demonstrated the expression of the CD134L molecule on rat DC. CD134L, recognized by the OX40L MAb, was

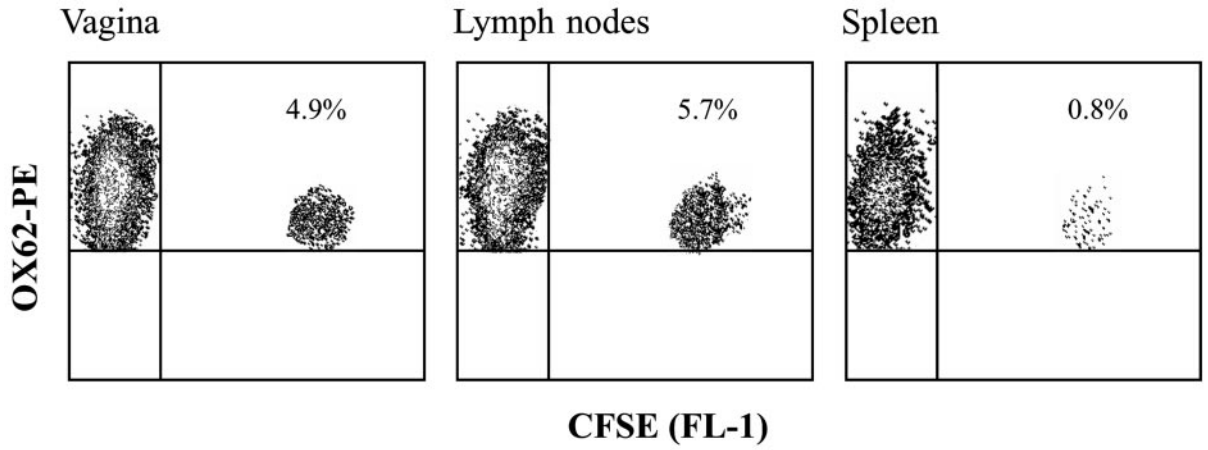

FIG. 7. Flow cytometric analysis of spleen, lymph node, and vaginal mucosa OptiPrep gradient-separated DCs from oophorectomized estradiol-treated noninfected rats 48 h after adoptive transfer of CFSE-labeled VDCs. A total of 1×10^5 enriched VDCs from rats infected with *Candida* for 2 weeks were labeled with CFSE and injected intravenously. The percentage of CFSE-positive cells was evaluated on DCs isolated from the different tissues after staining with PE-conjugated OX62 MAb by flow cytometry. The right, middle, and left panels represent the percentage of $OX62^+$ $CFSE^+$ VDCs on vaginal mucosa, lymph node, and spleen from noninfected rats, after gating on $OX62^+$ cells for acquisition. Data are for two separate experiments; the numbers represent the percentage of $OX62^+$ $CFSE^+$ VDCs.

specifically induced on $CD5^-$ $CD4^-$and on $CD5^+$ $CD4^+$ $CD86^+$ $CD80^+$ VDC subsets after *Candida* infection. CD134L is a type II membrane protein belonging to the TNF receptor-TNF superfamily involved in the generation of memory T-cell recall responses (11) and is required for optimal B-cell responses (28). CD134L is not constitutively expressed by resting or immature human antigen-presenting cells (APC) but can be induced in 24 h to several days on a number of cell types, including B cells and DCs (1, 35, 46). In the rat, CD134L is expressed on splenic B cells after stimulation with lipopolysaccharide, but not on peritoneal macrophages or resting and activated T cells (43). CD134L can provide a CD28-independent costimulatory signal to T cells (1). The CD134-CD134L interaction enhances T-cell proliferation and production of both Th1 (IL-2, TNF-α, and IFN-γ) and Th2 (IL-4, IL-10, and IL-13) cytokines (25, 36, 43).

The result of encounters between antigen-bearing APCs and naïve T cells depends partly on the nature of the cytokines locally released by APCs. The analysis of cytokines released from the distinct $OX62^+$, $CD4^+$ $CD5^+$ $CD86^+$ $CD80^+$ $CD134L^+$, $CD4^+$ $CD5^+$ $CD86^+$ $CD80^-$ $CD134L^-$, and $CD4^-$ $CD5^-$ $CD86^-$ $CD80^-$ $CD134L^+$ VDC subsets indicates that *C. albicans* infection stimulates all of the subsets that can produce IL-12, TNF-α, IL-2, and IL-10, with a preferential production of inflammatory cytokines TNF-α and IL-12 by the $CD4^-$ VDC subset.

These results are in accordance with previous evidence showing that in the rat (50) the splenic $CD4^-$ DC subset can produce large amounts of IL-12 and TNF-α, whereas the $CD4^+$ DC population produces small amounts of IL-12 and no TNF-α (50). IL-12 is both required and prognostic for Th1 development in mice with *Candida albicans* infection (39), and in fact IL-12-deficient mice are highly susceptible to gastrointestinal infection or to *Candida* reinfection (29). Furthermore, ingestion of *Candida* yeasts by activated murine DCs, induces IL-12 production and Th1 priming, whereas ingestion of hyphae inhibits IL-12 and Th1 priming and induces IL-4 production (17). In addition, *Candida* yeast cells trigger human DCs to produce low levels of IL-10 as compared to germ-tube cells, but comparable IL-12p70 levels (38). TNF-α is also involved in the successful control of *Candida* infection and the development of Th1-dependent response. By using TNF-α-knockout mice, impaired neutrophil recruitment and phagocytosis of *Candida* in animals lacking TNF-α has been observed (32). Furthermore, highly purified $OX62^+$ VDCs from *C. albicans*-infected rats produced a low level of IL-2; similarly, a bacterial encounter induces IL-2 secretion by murine DCs (22); which is the role of DC-derived IL-2 in vaginal candidiasis has not been addressed. It has been suggested (22) that early activated IL-2-deficient DCs were severely impaired in their ability to induce allogeneic $CD4^+$ and $CD8^+$ T-cell proliferation compared with wild-type DCs and a role of DC-derived IL-2 in the activation of NK and B-cell responses.

In accordance with the repertoire of costimulatory molecules and cytokine released, our results also provide evidence that VDCs from *C. albicans*-infected rats but not from noninfected rats are capable of activating syngeneic naïve $CD4^+$ T cells to release cytokines, namely IFN-γ, IL-2, IL-6, and IL-10, in response to the superantigen SEB, suggesting that they can play a crucial role in eliciting in vivo an anti-*Candida* T-cell-mediated protective immune response. Similar to our observations, submucosal VDCs are reported to elicit a protective IFN-γ-mediated $CD4^+$ T-cell response to herpes simplex virus type 2 (51).

Our study also provides direct evidence of the ability of VDCs to induce anti-*Candida* protective immunity by in vivo adoptive transfer of freshly isolated highly purified $OX62^+$ cells. VDCs isolated from infected rats induced a state of antifungal resistance, as revealed by significantly decreased and delayed fungal growth. These VDCs seem to be highly efficient, as demonstrated by the fact that a single inoculation of a relatively low number of VDCs from infected rats, given 1 day before challenge, was sufficient to achieve a substantial degree of protection against *Candida* infection. Infected VDC-mediated protection was associated with their ability to rapidly migrate to the vaginal mucosa and lymph nodes, as assessed by adoptive transfer of CFSE-labeled VDCs.

While our study emphasized the protective role of VDCs against vaginal candidiasis, the exact mechanisms whereby these cells confer protection are far from being defined. The rapid protection against *Candida* infection observed following VDC adoptive transfer strongly supports the involvement of innate immunity effector mechanisms, including direct elimination of the yeast by VDCs that are endowed with phagocytic and killing capability and/or activation of other innate immune cells, such as macrophages, in response to VDC-derived inflammatory cytokines. In this regard, human and murine DCs phagocytose, kill, and process *Candida* (17, 34, 38) and IL-12- and TNF-α-activated neutrophils and macrophages exert potent candidacidal activity (9).

On the other hand, the evidence that VDCs migrate into draining lymph nodes, together with their ability to prime T cells, suggests their potential role in a long-lasting protective effect mediated by adaptive immunity effector mechanisms. We have previously reported (42) the capability of vaginal lymphocytes, and in particular purified $CD4^+$ T cells, that are adoptively transferred to protect noninfected rats from *Candida* infection. In this respect, the $CD4^+$ $CD80^+$ $CD86^+$ $CD134L^+$ and $CD4^-$ $CD80^-$ $CD86^-$ $CD134L^+$ dendritic cells present in the vagina of *Candida*-infected rats could represent the major APCs involved in the transmission of the CD28/CD134-dependent, CD28-independent/CD134-dependent, or both costimulatory signals leading to activation, clonal expansion, and effector functions of *Candida* antigen-specific $CD4^+$ T cells. There is much evidence to support this hypothesis: the increased number of activated $CD4^+$ $CD25^+$ vaginal T cells; the presence of Th1 cytokines, namely IL-2, IL-12, and IFN-γ found in the vaginal fluids of *Candida*-infected rats (13); the restricted expression of CD134, the receptor for the CD134 ligand on activated $CD4^+$ $CD25^+$ T cells; and the abrogation of $CD4^+$ T-cell responses in CD134- or CD134L-deficient mice (43).

We have also previously reported the presence of IgM and IgG Abs directed against mannan constituents and aspartyl proteinase(s) of *Candida* (13) in the vaginal fluids of *Candida*-resistant rats and the capability of these vaginal fluids to passively transfer anti-*Candida* protection to noninfected rats (10). In addition, we have also described increased $CD3^-$ $CD5^+$ B-cell numbers and the ability of these B cells to protect noninfected rats from *Candida* infection (5), although at lower

levels of $CD4^+$ T cells (42). It has been shown that T helper 2 and B-cell differentiation depends on B7-CD28 costimulation and is enhanced by CD134-CD134L interaction (47). Thus, the VDC subset expressing the CD80/CD86/CD134L costimulatory molecules may contribute to the generation of signals leading to the differentiation of B cells and the production of anti-*Candida* Abs.

Finally, in vivo cytokines secreted by distinct VDC subsets after *Candida* infection could also play an important role in the induction of activation of innate immune effector cells and maintenance of anti-*Candida* immunity. Thus, IL-12 in addition to priming $CD4^+$ T cells toward an anti-*Candida* Th1 response, may also promote the maturation of naïve B cells into plasma cells secreting high levels of IgM and IgG Abs (16). Furthermore, optimal costimulation of IL-12-dependent $CD4^+$ Th1 cells may depend on IL-10 secretion by the immune VDCs.

No equivalent counterpart regarding the phenotype and function of VDCs has been provided so far, either in the mouse or human candidal vaginitis. Thus, as anti-*Candida* immune responses at the vaginal level are quite distinct in mice, rats, and humans, the relevance of VDCs in the control of vaginal candidiasis in species other than rats is presently unclear (17a).

In conclusion, our results indicate that different $OX62^+$ VDC subsets localize in the vaginal tissues of *C. albicans*-infected rats. In response to *Candida* infection, mature VDCs express a number of costimulatory molecules and acquire the ability to secrete IL-12, TNF-α, IL-2, and IL-10 cytokines. This efficiently primes syngeneic naïve $CD3^+$ $CD4^+$ T cells to antigen stimulation and, more importantly, when adoptively transferred in vivo can mediate protection against *C. albicans* vaginal infection.

ACKNOWLEDGMENTS

We are grateful to Angela Santoni for the critical reading of the manuscript and for providing useful suggestions. We would like to thank Antonietta Girolamo and Sofia Graziani for their contribution to the work described. We are also grateful to G. Mandarino for her valuable help with manuscript preparation.

This work was supported in part by the National AIDS Research Program under ISS contract 50F/C.

REFERENCES

1. **Akiba, H., H. Ohima, K. Takeda, M. Astuta, H. Nakano, A. Nakajima, C. Nohara, H. Yagita, and K. Okomura.** 1999. CD28-independent costimulation of T cells by OX40 ligand and CD70 on activated B cells. J. Immunol. **162:**7058–7066.
2. **Austyn, J. M.** 1998. Dendritic cells. Curr. Opin. Hematol. **5:**3–15.
3. **Bacci, A., C. Montagnoli, K. Perruccio, S. Bozza, R. Gaziano, L. Pitzurra, A. Velardi, C. F. d'Ostiani, J. E. Cutler, and L. Romani.** 2002. Dendritic cells pulsed with fungal RNA induce protective immunity to *Candida albicans* in hematopoietic transplantation. J. Immunol. **168:**2904–2913.
4. **Banchereau, J., and R. M. Steinman.** 1998. Dendritic cells and the control of immunity. Nature **329:**245–252.
5. **Banuls, M. P., A. Alvarez, I. Ferrero, A. Zapata, and C. Ardavin.** 1993. Cell-surface marker analysis of rat thymic dendritic cells. Immunology **79:** 298–304.
6. **Brenan, M., and M. Puklavec.** 1992. The MCR OX-62 antigen: a useful marker in the purification of rat veiled cells with the biochemical properties of an integrin. J. Exp. Med. **175:**1457–1465.
7. **Brenan, M., and J. Rees.** 2000. Sequence analysis of rat integrin a_{E1} and a_{E2} subunits: tissue expression reveals phenotypic similarities between intraepithelial lymphocytes and dendritic cells in lymph. Eur. J. Immunol. **30:**1527–1537.
8. **Buentke, E., and A. Scheynius.** 2003. Dendritic cells and fungi. APMIS **111:**789–796.
9. **Calderone, R. A.** 2002. Candida and candidiasis. ASM Press, Washington, D.C.
10. **Cassone, A., M. Boccanera, D Adriani, G. Santoni, and F. De Bernardis.** 1995. Rats clearing a vaginal infection by *Candida albicans* acquire specific, antibody-mediated resistance to vaginal reinfection. Infect. Immun. **63:**2619–2625.
11. **Croft, M.** 2003. Co-stimulatory members of the TNFR family: keys to effective T-cell immunity? Nat. Rev. Immunol. **3:**609–620.
12. **De Bernardis, F., M. Boccanera, D. Adriani, E. Spreghini, G. Santoni, and A. Cassone.** 1997. Protective role of antimannan and anti-aspartyl proteinase antibodies in an experimental model of *Candida albicans* vaginitis in rats. Infect. Immun. **65:**3399–3405.
13. **De Bernardis, F., G. Santoni, M. Boccanera, E. Spreghini, D. Adriani, L. Morelli, and A. Cassone.** 2000. Local anticandidal immune responses in a rat model of vaginal infection by and protection against *Candida albicans*. Infect. Immun. **68:**3297–3304.
14. **De Bernardis, F., M. Boccanera, D. Adriani, A. Girolamo, and A. Cassone.** 2002. Intravaginal and intranasal immunizations are equally effective in inducing vaginal antibodies and conferring protection against *Candida albicans*. Infect. Immun. **70:**2725–2729.
15. **Di Rosa, F., and A. Santoni.** 2003. Memory T-cell competition for bone marrow seeding. Immunology **108:**296–304.
16. **Dubois, B., C. Massacrier, B. Vanbervliet, J. Fayette, F. Brière, J. Banchereau, and C. Caux.** 1998. Critical role of IL-12 in dendritic cell-induced differentiation of naive B lymphocytes. J. Immunol. **161:**2223–2231.
17. **Fe d'Ostiani, C. F., G. Del Sero, A. Bacci, C. Montagnoli, A. Spreca, A. Mencacci, P. Ricciardi-Castagnoli, and L. Romani.** 2000. Dendritic cells discriminate between yeasts and hyphae of the fungus *Candida albicans*: implications for initiation of T helper cell immunity in vitro and in vivo. J. Exp. Med. **191:**1661–1673.

17a. **Fidel, P. L.** 2004. History and new insights into host defence against vaginal candidiasis. Trends Microbiol. **12:**220–227.

18. **Fidel, P. L., Jr., M. E. Lynch, D. H. Conaway, L. Tait, and J. D. Sobel.** 1995. Mice immunized by primary vaginal *Candida albicans* infection develop acquired vaginal mucosal immunity. Infect. Immun. **63:**547–553.
19. **Fidel, P. L., Jr., W. Luo, C. Steele, J. Chabian, M. Baker, and F. Wormley, Jr.** 1999. Analysis of vaginal cell populations during experimental vaginal candidiasis. Infect. Immun. **67:**3135–3140.
20. **Gaspari, A., R. Burns, A. Nasir, D. Ramirez, R. K. Barth, and C. G. Haidaris.** 1998. CD86 (B7-2), but not CD80 (B7-1), expression in the epidermis of transgenic mice enhances the immunogenicity of primary cutaneous *Candida albicans* infections. Infect. Immun. **66:**4440–4449.
21. **Granucci, F., C. Vizzardelli, E. Virzi, M. Rescigno, and P. Ricciardi-Castagnoli.** 2001. Transcriptional reprogramming of dendritic cells by differentiation stimuli. Eur. J. Immunol. **31:**2539–2546.
22. **Granucci, F., I. Zanoni, S. Feau, and P. Ricciardi-Castagnoli.** 2003. Dendritic cell regulation of immune responses: a new role for interleukin 2 at the intersection of innate and adaptative immunity. EMBO J. **22:**2546–2551.
23. **Huang, Q., D. Liu, P. Majewski, L. C. Schulte, J. M. Korn, R. A. Young, E. S. Lander, and N. Hacohen.** 2001. The plasticity of dendritic cell responses to pathogens and their components. Science **294:**870–875.
24. **Hubert, F. X., C. Voisine, C. Louvet, M. Heslan, and R. Josien.** 2004. Rat plasmacytoid dendritic cells are an abundant subset of MHC class $II^+CD4^+CD11b^-OX62^-$ and type I IFN-producing cells that exhibit selective expression of Toll-like receptors 7 and 9 and strong responsiveness to CpG. J. Immunol. **172:**7485–7494.
25. **Humphreys, I. R., L. Edwards, G. Walzi, A. J. Rae, G. Dougan, S. Hill, and T. Hussell.** 2003. OX40 ligation on activated T cells enhances the control of *Cryptococcus neoformans* and reduces pulmonary eosinophilia. J. Immunol. **170:**6125–6132.
26. **Lanzavecchia, A., and F. Sallusto.** 2001. Regulation of T cell immunity by dendritic cells. Cell **106:**263–266.
27. **Liu, L., M. Zhang, C. Jenkins, and G. G. MacPherson.** 1998. Dendritic cell heterogeneity in vivo: two functionally different dendritic cell populations in rat intestinal lymph can be distinguished by CD4 expression. J. Immunol. **161:**1146–1155.
28. **Malmstrom, V., D. Shipton, B. Singh, A. Al-Shamkhani, M. J. Puklavec, N. Barclay, and F. Powrie.** 2001. CD134L expression on dendritic cells in the mesenteric lymph nodes drives colitis in T-cell restored SCID mice. J. Immunol. **166:**6972–6981.
29. **Mencacci, A., E. Cenci, G. Del Sero, C. Fe d'Ostiani, P. Mosci, G. Trinchieri, L. Adorini, and L. Romani.** 1998. IL-10 is required for the development of protective Th1 responses in IL-12-deficient mice upon *Candida albicans* infection. J. Immunol. **161:**6228–6237.
30. **Mencacci, A., C. Montagnoli, A. Bacci, E. Cenci, L. Pitzurra, A. Spreca, M. Koft, A. H. Scarpe, and L. Romani.** 2002. $CD80^+$ $Gr\text{-}1^+$ myeloid cells inhibit development of antifungal Th1 immunity in mice with candidiasis. J. Immunol. **169:**3180–3190.
31. **Montagnoli, C., A. Bacci, S. Bozza, R. Gaziano, P. Mosci, A. H. Sharpe, and L. Romani.** 2002. B7/CD28-dependent $CD4^+CD25^+$ regulatory T cells are essential components of the memory-protective immunity to *Candida albicans*. J. Immunol. **169:**6298–6308.
32. **Netea, M. G., L. J. van Tits, J. H. Curfs, F. Amiot, J. F. Meis J. W. van der Meer, and B. J. Kullberg.** 1999. Increased susceptibility of TNF-alpha lym-

photoxin-alpha double knockout mice to systemic candidiasis through impaired recruitment of neutrophils and phagocytoses of *Candida albicans*. J. Immunol. **163:**1498–1505.
33. **Netea, M. G., R. Sutmuller, C. Hermann, C. A. A. Van der Graaf, J. W. M. Van der Meer, J. H. van Kricken, T. Hartung, G. Adema, and B. J. Kullberg.** 2004. Toll-like receptor 2 suppresses immunity against *Candida albicans* through induction of IL-10 and regulatory T cells. J. Immunol. **172:**3712–3718.
34. **Newman, S. L., and A. Holly.** 2001. *Candida albicans* is phagocytosed, killed, and processed for antigen presentation by human dendritic cells. Infect. Immun. **69:**6813–6822.
35. **Ohshima, Y., Y. Tanaka, H. Tozawa, Y. Takahashi, C. Maliszewski, and G. Delespesse.** 1997. Expression and function of OX40 ligand on human dendritic cells. J. Immunol. **159:**3838–3848.
36. **Ohshima, Y., L. P. Yiang, T. Uchiyama, Y. Tanaka, P. Baum, M. Sergerie, P. Hermann, and G. Delespesse.** 1998. OX40 costimulation enhances interleukin-4 (IL-4) expression at priming and promotes the differentiation of naïve human $CD4^+$ T cells into high IL-4-producing effectors. Blood **92:**3338–3345.
37. **Reis e Sousa, C., A. Sher, and P. Kaye.** 1999. The role of dendritic cells in the induction and regulation of immunity to microbial infection. Curr. Opin. Immunol. **11:**392–399.
38. **Romagnoli, G., R. Nisini, P. Chiani, S. Mariotti, R. Teloni, A. Cassone, and A. Torosantucci.** 2004. The interaction of human dendritic cells with yeast and germ-tube forms of *Candida albicans* leads to efficient fungal processing, dendritic cell maturation, and acquisition of a Th1 response-promoting function. J. Leukoc. Biol. **75:**117–126.
39. **Romani, L., A. Mencacci, L. Connetti, R. Spaccapelo, E. Cenci, S. Wolf, P. Puccetti, and F. Bistoni.** 1994. Interleukin-12 but not interferon-g production correlates with induction of T helper type-1 phenotype in murine candidiasis. Eur. J. Immunol. **53:**5157–5175.
40. **Romani, L., F. Bistoni, and P. Puccetti.** 2002. Fungi, dendritic cells and receptors: a host perspective of fungal virulence. Trends Microbiol. **10:**508–514.
41. **Romani, L., C. Montagnoli, S. Bozza, K. Perruccio, A. Spreca, P. Allavena, S. Verbeek, R. A. Calderone, F. Bistoni, and P. Puccetti.** 2004. The exploitation of distinct recognition receptors in dendritic cells determines the full range of host immune relationships with *Candida albicans*. Int. Immunol. **16:**149–161.
42. **Santoni, G., M. Boccanera, D. Adriani, R. Lucciarini, C. Amantini, S. Morrone, A. Cassone, and F. De Bernardis.** 2002. Immune cell-mediated protection against vaginal candidiasis: evidence for a major role of vaginal $CD4^+$ T cells and possible participation of other local lymphocyte effectors. Infect. Immun. **70:**4791–4797.
43. **Satake, Y., H. Akiba, K. Takeda, M. Atsuta, H. Yagita, and K. Okumura.** 2000. Characterization of rat OX40 ligand by monoclonal antibody. Biochem. Biophys. Res. Commun. **270:**1041–1048.
44. **Sobel, J. D.** 1992. Pathogenesis and treatment of recurrent vulvovaginal candidiasis. Clin. Infect. Dis. **14:**148–153.
45. **Steinman, R. M., S. Turley, I. Mellman, and K. Inaba.** 2000. The induction of tolerance by dendritic cells that have captured apoptotic cells. J. Exp. Med. **191:**411–416.
46. **Stuber, E., M. Neurath, D. Calderhead, H. Fell, and W. Strober.** 1995. Cross-linking of OX40 ligand, a member of the TNF/NGF cytokine family, induces proliferation and differentiation in murine splenic cells. Immunity **2:**507–521.
47. **Tanaka, H., C. E. Demeure, M. Rubio, G. Delespesse, and M. Sarfati.** 2000. Human monocyte-derived dendritic cells induce naive T cell differentiation into T helper cell type 2 (Th2) or Th1/Th2 effectors. Role of stimulator/responder ratio. J. Exp. Med. **192:**405–412.
48. **Torosantucci, A., G. Romagnoli, P. Chiani, A. Stringaro, P. Crateri, S. Mariotti, R. Teloni, G. Arancia, A. Cassone, and R. Nisini.** 2004. *Candida albicans* yeast and germ tube forms interfere differently with human monocyte differentiation into dendritic cells: a novel dimorphism-dependent mechanism to escape the host's immune response. Infect. Immun. **72:**833–843.
49. **Trinite, B., C. Voisine, H. Yagita, and R. Josien.** 2000. A subset of cytolytic dendritic cells in rat. J. Immunol. **165:**4202–4208.
50. **Voisine, C., F. X. Hubert, B. Trinité, M. Heslan, and R. Josien.** 2002. Two phenotypically distinct subsets of spleen dendritic cells in rats exhibit different cytokine production and T cell stimulatory activity. J. Immunol. **169:**2284–2291.
51. **Zhao, X., E. Deak, K. Soderberg, M. Linehan, D. Spezzano, J. Zhu, D. M. Knipe, and A. Iwasaki.** 2003. Vaginal submucosal dendritic cells, but not Langerhans cells, induce protective Th1 responses to *Herpes Simplex Virus-2*. J. Exp. Med. **197:**153–162.

Editor: A. Casadevall